Articles

Impact of Steric Blocking on Diastereoselective C−H Activation of Ethylbenzene by Cationic Platinum(II) Complexes with 7-Azaindolyl Derivative Ligands

Shu-Bin Zhao, Gang Wu, and Suning Wang*

Department of Chemistry, Queen's University, Kingston, Ontario K7L 3N6, Canada

Received September 27, 2006

Ethylbenzene C−H activation reactions using the cationic compounds $[Pt(BAB)(CH_3)(L)]^+$ and $[Pt(BAM)(CH_3)(L)]^+$ generated in situ by the reaction of $[(Et_2O)_2H][BAr'_4]$ with the parent molecules $Pt(BAB)(CH_3)_2$ (**1**) and $Pt(BAM)(CH_3)_2$ (**2**), respectively, have been examined (BAB = 1,2-bis(*N*-7-azaindolyl)benzene, BAM = bis(*N*-7-azaindolyl)methane). The impact of the steric blockage of the Pt axial coordination site by the BAB and BAM ligands on the regio- and diastereoselectivity of the ethylbenzene C−H activation has been investigated. For both Pt complexes the benzylic C−H activation products were found to be thermodynamically favored, with the BAB complex showing a higher regioselectivity. In addition, both complexes display distinct diastereoselectivity in the formation of the η^1-benzylic products $[Pt(BAB)(CH_3CN)(CH(Me)Ph)][BAr'_4]$ (**3**) and $[Pt(BAM)(CH_3CN)(CH(Me)Ph)][BAr'_4]$ (**4**), with the BAB complex showing a much higher diastereoselectivity. The structures of the diastereomers have been established by single-crystal X-ray diffraction and 2D NOESY NMR analyses. The two η^3 complexes $[Pt(BAB)(\eta^3\text{-}CH(Me)Ph)][BAr'_4]$ (**5**) and $[Pt(BAM)(\eta^3\text{-}CH(Me)Ph)][BAr'_4]$ (**6**) have been characterized, and the structure of **5** has been determined by single-crystal X-ray diffraction analysis. The η^3 complexes have been found to exist in two isomeric forms, with one isomer being dominant. NMR experiments established that the η^3 complexes **5** and **6** can be converted quantitatively to the corresponding η^1 complexes **3** and **4**, respectively, with the retention of the isomer (or diastereomer) ratio. The results of this investigation are consistent with the η^3-benzylic complex being the reaction intermediate in the formation of the η^1-benzylic complex. The asymmetric blocking of the Pt axial coordination site by the BAB and BAM ligands was found to be responsible for the observed diastereoselectivity in ethylbenzene C−H activation.

Introduction

Selective activation of inert C−H bond by transition-metal compounds is a key step toward catalytic and direct hydrocarbon functionalization.[1] Since the demonstration of the catalytic transformation of CH_4 into CH_3OH and CH_3Cl by Pt(II)/Pt(IV) salts in aqueous systems by Shilov and co-workers,[2] considerable research efforts have been directed to the study and understanding of the electrophilic C−H activation process on a Pt center by using a variety of organoplatinum model systems, and extensive investigations on the key steps involved in alkane C−H bond activation on a Pt(II) center have been conducted and valuable new insights on the role of the Pt(II) center have been obtained.[3] The electronic and steric impacts on the kinetic and thermodynamic selectivity of alkylarene C−H activation have been the focus of several recent reports involving cationic Pt(II) compounds.[4−8] Previous studies on various Pt(II) model systems by a number of research groups[5−7] have consistently demonstrated a high kinetic preference for aryl C−H activation. Investigation by the Tilset and Bercaw groups on C−H activation using Pt(II) complexes containing diimine ligands with the general formula Ar′N═C(R)C(R)═NAr′ revealed that the formation of the thermodynamically preferred benzylic products initially competes effectively with that of the kinetically preferred aromatic products.[5c,6k,j] For aryl C−H

* To whom correspondence should be addressed. E-mail: wangs@chem.queensu.ca.

(1) (a) Goldberg, K. I.; Goldman, A. S. *Activation and Functionalization of C-H Bonds*; American Chemical Society: Washington, DC, 2004. (b) Janowicz, A. H.; Bergman, R. G. *J. Am. Chem. Soc.* **1982**, *104*, 352; **1983**, *105*, 3929. (c) Jones, W. D.; Feher, F. J. *J. Am. Chem. Soc.* **1984**, *106*, 1650. (d) Chen, H. Y.; Schlecht, S.; Semple, T. C.; Hartwig, J. F. *Science* **2000**, *287*, 1995.

(2) (a) Goldshlegger, N. F.; Tyabin, M. B.; Shilov, A. E.; Shteinman, A. A. *Zh. Fiz. Khim.* **1969**, *43*, 2174. (b) Goldshlegger, N. F.; Eskova, V. V.; Shilov, A. E.; Shteinman, A. A. *Zh. Fiz. Khim.* **1972**, *46*, 1353.

(3) For recent comprehensive reviews on cationic Pt(II)-mediated C−H bond activation studies, see: (a) Arndtsen, B. A.; Bergman, R. G.; Mobley, T. A.; Peterson, T. H. *Acc. Chem. Res.* **1995**, *28*, 154. (b) Bengali, A. A.; Arndtsen, B. A.; Burger, P. M.; Schultz, R. H.; Weiller, B. H.; Kyle, K. R.; Moore, C. B.; Bergman, R. G. *Pure Appl. Chem.* **1995**, *67*, 281. (c) Crabtree, R. H. *Chem. Rev.* **1995**, *95*, 987. (d) Shilov, A. E.; Shulpin, G. B. *Chem. Rev.* **1997**, *97*, 2879. (e) Shilov, A. E.; Shul'pin, G. B. *Chem. Rev.* **1997**, *97*, 2879. (f) Stahl, S. S.; Labinger, J. A.; Bercaw, J. E. *Angew. Chem., Int. Ed.* **1998**, *37*, 2180. (g) Labinger, J. A.; Bercaw, J. E. *Nature* **2002**, *417*, 507. (h) Fekl, U.; Goldberg, K. I. *Adv. Inorg. Chem.* **2003**, *54*, 259. (i) Lersch, M.; Tilset, M. *Chem. Rev.* **2005**, *105*, 2471.

(4) (a) Periana, R. A.; Taube, J. D.; Gamble, S.; Taube, H.; Satoh, T.; Fujii, H. *Science* **1998**, *280*, 560. (b) Sen, A. *Acc. Chem. Res.* **1998**, *31*, 550. (c) Ziatdinov, V. R.; Oxgaard, J.; Mironov, O. A.; Young, K. J. H.; Goddard, W. A., III; Periana, R. A. *J. Am. Chem. Soc.* **2006**, *128*, 7404.

10.1021/om0608861 CCC: $33.50
Publication on Web 11/16/2006

Chart 1

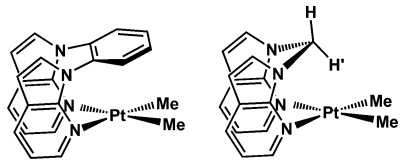

Pt(BAB)$(CH_3)_2$, **1** Pt(BAM)$(CH_3)_2$, **2**

activation products, the kinetic preference of para and meta C−H activation was observed and they were found to undergo transformation to the benzylic C−H activation products.[6k,j] For some of the alkyl-substituted benzenes, this regiospecific selectivity has been attributed to the thermodynamic stability of a η^3-benzylic complex characterized by NMR spectroscopic analyses, which can be converted cleanly to the η^1-benzylic product upon the addition of donor ligands such as acetonitrile.[6j]

The majority of previous investigations on C−H activation involving cationic Pt(II) centers have focused on regioselectivity. Information on stereo- or diastereoselective C−H bond activation using Pt complexes has been rather scarce, except for the few recent examples reported by Sames and co-workers, where cationic Pt(II) complexes with chiral auxiliary ligands were used in stereoselective C−H activation.[10,11] We have reported recently that cationic Pt(II) complexes containing 7-azaindolyl derivative ligands such as BAB (1,2-bis(*N*-7-azaindolyl)benzene) and *N*,*N*-bis(7-azaindolyl)methane (BAM) as shown in Chart 1 can undergo facile C−H activation with benzene or toluene.[12] In case of toluene, the Pt(BAB)$(CH_3)_2$ compound (**1**) was found to activate toluene C−H bonds regioselectively with the benzylic product as the dominating product,[12a] consistent with the behavior of the diimine Pt(II) complexes investigated by Bercaw and co-workers.[6k,j] The key feature of the BAM and BAB ligands is that they cap the fifth coordination site of the Pt(II) center. Because of the different sizes of the linkers in BAB (phenyl) and BAM (CH_2), this pair of ligands provides us a unique opportunity to investigate the impact of steric blocking of the Pt axial coordination site on the regio- and diastereoselectivity of alkylbenzene C−H bond activation. We have examined the reactions of ethylbenzene with Pt(BAB)$(CH_3)_2$ and Pt(BAM)$(CH_3)_2$. We have observed that, in addition to regioselectivity, the reactions of ethylbenzene with these two Pt(II) compounds display a distinct and contrasting diastereoselectivity, a phenomenon that has not been reported in other cationic Pt(II) systems with the exception of intramolecular chiral auxiliary ligand mediated C−H activation systems.[10,11] In addition, we have succeeded in isolating and structurally characterizing a key η^3-benzylic complex, identifying the coexistence of two η^3 structural isomers, and determining their role in diastereoselective ethylbenzene C−H bond activation. The details are presented herein.

Experimental Section

All reactions were performed under an inert atmosphere of dry N_2 with standard Schlenk techniques or in a drybox. Solvents were freshly distilled prior to use. ^{1}H NMR and ^{13}C NMR spectra were recorded on Bruker Avance 400 or 500 spectrometers, and the spectra were referenced to residual solvent peaks. Elemental analyses were performed by Canadian Microanalytical Service, Ltd, Delta, British Columbia. Starting materials were purchased from Aldrich Chemical Co. and used without further purification. $[H(Et_2O)_2][BAr'_4]$ (Ar′ = 3,5-bis(trifluoromethyl)phenyl) was prepared using a procedure reported in the literature.[13] Pt(BAB)$(CH_3)_2$ and Pt(BAM)$(CH_3)_2$ were synthesized as reported previously.[12]

Ethylbenzene C−H Activation by Pt(BAB)$(CH_3)_2$ (1) and the Isolation of [Pt(BAB)(CHMePh)(MeCN)][BAr′$_4$] (3). Under N_2, $[H(Et_2O)_2][BAr'_4]$ (190 mg, 0.19 mmol) was added to a stirred solution of Pt(BAB)$(CH_3)_2$ (100 mg, 0.19 mmol) in ethylbenzene (20.0 mL) at ambient temperature (22 °C). The solution mixture became clear and turned pink in ∼1 min. During the reaction, thick brown oily residue accumulated slowly on the bottom of the flask. After 5 days, CH_3CN (0.20 mL, 3.8 mmol) was added to terminate the reaction. After the reaction mixture was stirred for another 1 h, the solution was separated from the oily residue (∼24 mg). The solvents were removed under vacuum. To remove ethylbenzene, the residue was repeatedly dissolved in CH_2Cl_2 and the solvent was repeatedly removed under vacuum (three times), which produced a brown residue of ∼260 mg. ^{1}H NMR analyses indicated that >90% of the products are η^1-benzylic C−H activation products along with aromatic C−H activation products (<10%) (^{1}H NMR spectrum of the oily residue showed the same composition as that of the bulk product.). Two sets of chemical shifts corresponding to the two diastereomers of the η^1-benzylic product with a ratio of ∼3.7:1 were observed in the ^{1}H NMR spectrum. Colorless crystals of **3** were obtained by recrystallization of the crude product from hexanes/THF (4/1). Anal. Calcd for $C_{62}H_{38}N_5BF_{24}Pt$: C, 49.16; H, 2.53; N, 4.62. Found: C, 48.50; H, 2.55; N, 4.55. ^{1}H NMR (400 MHz, CD_2Cl_2, 25 °C): major diastereomer, 8.34 (dd; ^3J = 5.4 Hz, ^4J = 1.1 Hz; 1H, aza), 8.05−7.91 (m; 3H, aza), 7.84−7.76 (m;

(5) (a) Johansson, L.; Ryan, O. B.; Tilset, M. *J. Am. Chem. Soc.* **1999**, *121*, 1974. (b) Johansson, L.; Tilset, M. *J. Am. Chem. Soc.* **2001**, *123*, 739. (c) Johansson, L.; Ryan, O. B.; Rømming, C.; Tilset, M. *J. Am. Chem. Soc.* **2001**, *123*, 6579. (d) Wik, B. J.; Lersch, M.; Tilset, M. *J. Am. Chem. Soc.* **2002**, *124*, 12116. (e) Wik, B. J.; Ivanovic-Burmazovic, I.; Tilset, M.; van Eldik, R. *Inorg. Chem.* **2006**, *45*, 3613. (f) Wik, B. J.; Lersch, M.; Krivokapic, A.; Tilset, M. *J. Am. Chem. Soc.* **2006**, *128*, 2682.

(6) (a) Luinstra, G. A.; Wang, L.; Stahl, S. S.; Labinger, J. A.; Bercaw, J. E. *J. Organomet. Chem.* **1995**, *504*, 75. (b) Stahl, S. S.; Labinger, J. A.; Bercaw, J. E. *J. Am. Chem. Soc.* **1996**, *118*, 5961. (c) Holtcamp, M. W.; Labinger, J. A.; Bercaw, J. E. *J. Am. Chem. Soc.* **1997**, *119*, 848. (d) Holtcamp, M. W.; Henling, L. M.; Day, M. W.; Labinger, J. A.; Bercaw, J. E. *Inorg. Chim. Acta* **1998**, *270*, 467. (e) Johansson, L.; Tilset, M.; Labinger, J. A.; Bercaw, J. E. *J. Am. Chem. Soc.* **2000**, *122*, 10846. (f) Procelewska, J.; Zahl, A.; van Eldik, R.; Zhong, H. A.; Labinger, J. A.; Bercaw, J. E. *Inorg. Chem.* **2002**, *41*, 2808. (g) Zhong, H. A.; Labinger, J. A.; Bercaw, J. E. *J. Am. Chem. Soc.* **2002**, *124*, 1378. (h) Wong-Foy, A. G.; Henling, L. M.; Day, M.; Labinger, J. A.; Bercaw, J. E. *J. Mol. Catal. A: Chem.* **2002**, *189*, 3. (i) Heyduk, A. F.; Labinger, J. A.; Bercaw, J. E. *J. Am. Chem. Soc.* **2003**, *125*, 6366. (j) Iverson, C. N.; Carter, C. A. G.; Baker, R. T.; Scollard, J. D.; Labinger, J. A.; Bercaw, J. E. *J. Am. Chem. Soc.* **2003**, *125*, 12674. (k) Heyduk, A. F.; Driver, T. G.; Labinger, J. A.; Bercaw, J. E. *J. Am. Chem. Soc.* **2004**, *126*, 15034. (l) Driver, T. G.; Day, M. W.; Labinger, J. A.; Bercaw, J. E. *Organometallics* **2005**, *24*, 3644. (m) Owen, J. S.; Labinger, J. A.; Bercaw, J. E. *J. Am. Chem. Soc.* **2006**, *128*, 2005.

(7) (a) Hill, G. S.; Manojlovic-Muir, L.; Muir, K. W.; Puddephatt, R. J. *Organometallics* **1997**, *16*, 525. (b) Prokopchuk, E. M.; Jenkins, H. A.; Puddephatt, R. J. *Organometallics* **1999**, *18*, 2861. (c) Hinman, J. G.; Baar, C. R.; Jennings, M. C.; Puddephatt, R. J. *Organometallics* **2000**, *19*, 563. (d) Zhang, F.; Kirby, C. W.; Hairsine, D. W.; Jennings, M. C.; Puddephatt, R. J. *J. Am. Chem. Soc.* **2005**, *127*, 14196.

(8) (a) Wick, D. D.; Goldberg, K. I. *J. Am. Chem. Soc.* **1997**, *119*, 10235. (b) Thomas, J. C.; Peters, J. C. *J. Am. Chem. Soc.* **2001**, *123*, 5100. (c) Konze, W. V.; Scott, B. L.; Kubas, G. J. *J. Am. Chem. Soc.* **2002**, *124*, 12550. (d) Thomas, J. C.; Peters, J. C. *J. Am. Chem. Soc.* **2003**, *125*, 8870. (e) Thomas, C. M.; Peters, J. C. *Organometallics* **2005**, *24*, 5858. (f) Karshtedt, D.; McBee, J. L.; Bell, A. T.; Tilley, T. D. *Organometallics* **2006**, *25*, 1801.

(9) For an example review on ortho-metalated transition-metal complexes, see: Mohr, F.; Privér, S. H.; Bhargava, S. K.; Bennett, M. A. *Coord. Chem. Rev.* **2006**, *250*, 1851.

(10) (a) Johnson, J. A.; Sames, D. *J. Am. Chem. Soc.* **2000**, *122*, 6321. (b) Johnson, J. A.; Li, D.; Sames, D. *J. Am. Chem. Soc.* **2002**, *124*, 6900.

(11) Dangel, B. D.; Johnson, J. A.; Sames, D. *J. Am. Chem. Soc.* **2001**, *123*, 8149.

(12) (a) Zhao, S. B.; Song, D.; Jia, W. L.; Wang, S. *Organometallics* **2005**, *24*, 3290. (b) Song, D.; Wang, S. *Organometallics* **2003**, *22*, 2187.

(13) Brookhart, M.; Grant, B.; Volpe, J. *Organometallics* **1992**, *11*, 3920.

2H, phenyl of 1,2-BAB), 7.74 (s; 8H, BAr′$_4$), 7.57 (s; 4H, BAr′$_4$), 7.46 (dd; ^3J = 8.0 Hz,^4J = 1.6 Hz; 1H, phenyl of 1,2-BAB), 7.42 (dd; ^3J = 8.0 Hz, ^4J = 2 Hz; 1H, phenyl of 1,2-BAB), 7.25 (d; ^3J = 3.6 Hz; 1H, aza), 7.23 (d; ^3J = 3.6 Hz; 1H, aza), 7.19−7.17 (m; 3H, Pt−CHMe*Ph*), 7.09 (dd; $^3J_1$ = 5.6 Hz, $^3J_2$ = 8.0 Hz; 1H, aza), 6.96 (dd; $^3J_1$ = 5.6 Hz, $^3J_2$ = 8.0 Hz; 1H, aza), 6.93−6.90 (m; 2H, Pt−CHMe*Ph*), 6.66 (d; ^3J = 3.6 Hz; 1H, aza), 6.63 (d; ^3J = 3.6 Hz; ^{1}H, aza), 3.33 (q, satellite; ^3J = 7.3 Hz, $^2J_{Pt-H}$ = 103.7 Hz; 1H, Pt−*CH*MePh), 2.22 (s; 3H, Pt−NC*Me*), 0.83 (d; ^3J = 7.3 Hz, $^3J_{Pt-H}$ = 50.4 Hz; 3H, Pt−CH*Me*Ph); minor diastereomer, 8.26 (dd; ^3J = 5.4 Hz,^4J = 1.1 Hz; 1H, aza), 8.05−7.91 (m; 5H, 3H from aza, 2H from phenyl of 1,2-BAB), 7.74 (s; 8H, BAr′$_4$), 7.60 (dd; ^3J = 8.0 Hz, ^4J = 1.6 Hz; 1H, phenyl of 1,2-BAB), 7.57 (s; 4H, BAr′$_4$), 7.51 (dd; ^3J = 8.0 Hz, ^4J = 1.6 Hz; 1H, phenyl of 1,2-BAB), 7.29 (d; ^3J = 3.6 Hz; 1H, aza), 7.27 (d; ^3J = 3.6 Hz; 1H, aza), 7.19−7.17 (m; 3H, Pt−CHMe*Ph*), 7.06 (dd, $^3J_1$ = 5.6 Hz, $^3J_2$ = 8.0 Hz; 1H, aza), 6.93−6.90 (m; 3H, 1H from aza, 2H from Pt−CHMe*Ph*), 6.68 (d; ^3J = 3.6 Hz; 1H, aza), 6.64 (d; ^3J = 3.6 Hz; ^{1}H, aza), 2.90 (q, satellite; ^3J = 7.3 Hz, $^2J_{Pt-H}$ = 103.7 Hz; 1H, Pt−*CH*MePh), 2.23 (s; 3H, Pt−NC*Me*), 0.89 (d, satellite; ^3J = 7.3 Hz, $^3J_{Pt-H}$ = 50.4 Hz; 3H, Pt−CH*Me*Ph). ^{13}C{^{1}H} NMR of all diastereomers (100 MHz, CD_2Cl_2; not fully assigned due to the complexity of the spectrum): BAr′$_4$ 162.9 (q, J_{B-H} = 50.1 Hz), 135.2 (br), 129.4 (q, br; J_{C-F} = 36 Hz), 125.3 (q; J_{C-F} = 272 Hz), 117.92 (br); 146.01, 145.97, 144.38, 144.30, 144.18, 144.12, 132.71, 132.57, 132.49, 132.34, 131.96, 131.87, 131.71, 131.54, 131.43, 131.31, 129.8, 129.40, 128.71, 128.60, 128.22, 124.90, 124.71, 123.8, 121.7, 117.89, 117.76, 104.17, 104.08; Pt−*CH*MePh (15.97, 14.45), Pt−CH*Me*Ph (14.58, 14.30), Pt−NC*Me* (3.53, 3.49).

Ethylbenzene C−H Activation by Pt(BAM)(CH$_3$)$_2$ (2) and the Isolation of [Pt(BAM)(CHMePh)(MeCN)][BAr′$_4$] (4). Under N_2, [H(Et$_2$O)$_2$][BAr′$_4$] (303 mg, 0.30 mmol) was added to a stirred solution of **2** (142 mg, 0.30 mmol) in ethylbenzene (25 mL) at ambient temperature (22 °C). A clear yellow solution was formed immediately. After 5 days, CH_3CN (0.60 mL, 11.4 mmol) was added and the reaction mixture was stirred for another 1 h. After the solvents were removed under vacuum, CH_2Cl_2 (5.0 mL) was used to dissolve the residue and then removed under vacuum. This was repeated three times to remove the ethylbenzene. A 392 mg amount of pale yellow residue was obtained. ^{1}H NMR analyses showed the presence of the benzylic C−H activation products as the major products (∼75%), along with aromatic C−H activation products (∼25%). The benzylic product displayed two sets of signals with a ratio of ∼1.5:1, corresponding to the two diastereomers in the ^{1}H NMR spectrum. The crystalline compound **4** was isolated from the reaction mixture after slow evaporation of the solvent. Anal. Calcd for $C_{57}H_{36}N_5BF_{24}Pt$: C, 47.12; H, 2.50; N, 4.82. Found: C, 47.18; H, 2.56; N, 4.72. ^{1}H NMR (400 MHz, CD_2Cl_2, 25 °C): minor diastereomer, 10.01 (d; ^2J = 15.4 Hz; 1H, CH_2 bridge), 8.47 (dd, br; $^3J_1$ = 5.4 Hz,$^3J_2$ = 1.0 Hz; 2H, aza), 8.08−8.00 (m, satellite; $^3J_{Pt-H}$ = 38.2 Hz; 2H, aza), 7.75 (s; 8H, BAr′$_4$), 7.58 (s; 4H, BAr′$_4$), 7.48−7.40 (m; 2H, aza), 7.22−7.15 (m; 2H, aza), 7.09−6.95 (m; 3H, Pt−CHMe*Ph*), 6.76−6.70 (m; 2H, Pt−CHMe*Ph*), 6.60−6.57 (m; 2H, aza), 6.00 (d; ^2J = 15.3 Hz; 1H, CH_2), 3.32 (q, satellite; ^3J = 7.2 Hz, $^2J_{Pt-H}$ = 109.3 Hz; 1H, Pt−*CH*MePh), 2.38 (s; 3H, Pt−NC*CH$_3$*), 1.40 (d, satellite; ^3J = 7.2 Hz, $^3J_{Pt-H}$ = 44.8 Hz; 3H, Pt−CH*Me*Ph); major diastereomer, 10.32 (d; ^2J = 15.3 Hz; 1H, CH_2 bridge), 8.74 (dd, satellite; $^3J_1$ = 5.6 Hz, $^3J_2$ = 1.2 Hz, $^3J_{Pt-H}$ = 60.3 Hz; 2H, aza), 8.55 (dd, satellite; $^3J_1$ = 5.7 Hz, $^3J_2$ = 1.2 Hz, $^3J_{Pt-H}$ = 60.6 Hz; 1H, aza), 7.75 (s, 8H, BAr′$_4$), 7.58 (s, 4H, BAr′$_4$), 7.48−7.40 (m; 2H, aza), 7.22−7.15 (m; 2H, aza), 7.09−6.95 (m; 3H, Pt−CHMe*Ph*), 6.76−6.70 (m; 2H, Pt−CHMe*Ph*), 6.66 (d; ^3J = 3.4 Hz; 2H, aza), 6.14 (d; ^2J = 15.4 Hz; 1H, CH_2 bridge), 3.76 (q, satellite; ^3J = 7.2 Hz, $^2J_{Pt-H}$ = 110.0 Hz; 1H, Pt−*CH*MePh), 2.24 (s; 3H, Pt−NC*Me*), 1.17 (d, satellite;^3J = 7.2 Hz, $^3J_{Pt-H}$ = 36.3 Hz; 3H, Pt−CH*Me*Ph). ^{13}C-{^{1}H} NMR of all isomers (100 MHz, CD_2Cl_2; not fully assigned due to the complexity of the spectrum): BAr′$_4$ 162.2 (q, J_{B-H} = 50.4 Hz), 135.2 (br), 129.5 (q, br; J_{C-F} = 36 Hz), 125.3 (q; J_{C-F} = 272 Hz), 117.92 (br); 151.37, 151.20, 147.17, 146.93, 132.63, 132.62, 132.48, 129.92, 129.47, 128.75, 128.24, 126.07, 125.93, 125.52, 124.36, 123.90, 118.23, 117.90, 117.87, 117.84, 104.10, 103.59, 103.57, 56.00, 55.53; Pt−*CH*MePh (20.23, 16.58), Pt−CH*Me*Ph (21.07, 19.49), Pt−NC*Me* (4.13, 3.84).

General Procedure of the ^{1}H NMR Spectroscopic Analyses of the Reaction Mixture. Under N_2, [H(Et$_2$O)$_2$][BAr′$_4$] (1.0 equiv) was added to a stirred ethylbenzene solution of the Pt(II) complex **1** or **2** at ambient temperature (22 °C). A small amount of the reaction mixture, during the course of the reaction, was taken out at regular time intervals and put immediately into NMR tubes that contain CD_3CN. These samples were dried, and the residues were then analyzed by ^{1}H NMR spectroscopy by using CD_2Cl_2 as the solvent. The assignment of the chemical shifts to the reaction mixture is based on spectroscopic data of the isolated benzylic C−H activation product and the ^{1}H NMR spectrum of the para aromatic C−H activation product, which was synthesized independently (see the Supporting Information).

Synthesis of [Pt(BAB)(η^3-CHPhMe)][BAr′$_4$] (5). Under N_2, [H(Et$_2$O)$_2$][BAr′$_4$] (160 mg, 0.30 mmol) was added to a solution of **1** (317 mg, 0.31 mmol) in ethylbenzene (30 mL) and the solution was stirred at ambient temperature for 5 days. After the solution was concentrated to ∼5 mL under vacuum and kept in a refrigerator for several weeks, colorless crystals of the η^3 complex **5** were obtained in ∼73% yield. Anal. Calcd for $C_{60}H_{35}BF_{24}N_4Pt$·0.5(ethylbenzene): C, 50.34; H, 2.64; N, 3.67. Found: C, 50.81; H, 2.97; N, 3.54. ^{1}H NMR (400 MHz, CD_2Cl_2, 25 °C; the aromatic region is not fully assigned because of many overlapping peaks; assignments are based on a 2D-COSY spectrum): major isomer, 3.92 (d, satellite; ^3J = 6.0 Hz, $^3J_{Pt-H}$ = 36.8 Hz; 1H, ortho Pt−η^3-CHMe*Ph*), 1.88 (q, satellite; ^3J = 6.4 Hz, $^3J_{Pt-H}$ = 66.8 Hz; 1H, Pt−η^3-*CH*MePh), 1.03 (d; ^3J = 6.4 Hz; 3H, Pt−η^3-CH*Me*Ph); minor isomer, 6.09 (d, satellite; ^3J = 6.0 Hz, $^3J_{Pt-H}$ = 42.6 Hz; 1H, ortho Pt−η^3-CHMe*Ph*), 3.18 (q, satellite; ^3J = 6.6 Hz, $^3J_{Pt-H}$ = 68.4 Hz; 1H, Pt−η^3-*CH*MePh), 0.82 (d; ^3J = 6.6 Hz; 3H, Pt−η^3-CH*Me*Ph). ^{13}C{^{1}H} NMR (100 MHz, CD_2Cl_2; key chemical shifts for major isomer): 67.03 (satellite; $^2J_{Pt-C}$ = 118 Hz; ortho Pt−η^3-CHMe*Ph*), 38.16 (satellite; $^2J_{Pt-C}$ = 283 Hz; Pt−η^3-*CH*MePh), 13.95 (satellite; $^3J_{Pt-C}$ = 186 Hz; Pt−η^3-CH*Me*Ph); key chemical shifts for minor isomer, 70.11 (satellite; $^2J_{Pt-C}$ = 112 Hz; ortho Pt−η^3-CHMe*Ph*), 34.90 (satellite; $^3J_{Pt-C}$ = 288 Hz; Pt−η^3-*CH*MePh), 11.44 (satellite; $^3J_{Pt-C}$ = 196 Hz; Pt−η^3-CH*Me*Ph).

Synthesis of [Pt(BAM)(η^3-CHPhMe)][BAr′$_4$] (6). The η^3 complex **6** was synthesized by a method similar to that described for **5**. After 5 days, compound **6** was found to be the major product in the reaction mixture according to NMR data. However, pure crystalline complex **6** could not be isolated from the reaction mixture because of the oily nature of the final reaction mixture and its high solubility in common organic solvents. Compound **6** was characterized by NMR spectroscopic analyses. The ^{1}H NMR spectrum of the η^3 complex **6** is provided in the Supporting Information. ^{1}H NMR (400 MHz, CD_2Cl_2, 25 °C; the aromatic region is not fully assigned due to the overlaps of peaks): major isomer, 8.69 (d; ^2J = 15.2 Hz; 1H, CH_2 bridge), 5.98 (d, satellite; ^3J = 6.8 Hz, $^3J_{Pt-H}$ = 44.0 Hz; 1H, ortho Pt−η^3-CHMe*Ph*), 5.89 (d; ^2J = 15.2 Hz; 1H, CH_2 bridge), 3.29 (q, satellite; ^3J = 6.4 Hz, $^3J_{Pt-H}$ = 68.8 Hz; 1H, Pt−η^3-*CH*MePh), 1.05 (d; ^3J = 6.4 Hz; 3H, Pt−η^3-CH*Me*Ph); minor isomer, 9.85 (d; ^2J = 15.2 Hz; 1H, CH_2 bridge), 6.34 (d; ^2J = 15.2 Hz; 1H, CH_2 bridge), 5.82 (d, satellite; ^3J = 6.6 Hz,$^3J_{Pt-H}$ = 36.4 Hz; 1H, ortho Pt−η^3-CHMe*Ph*), 3.20 (q, satellite; ^3J = 6.6 Hz, $^3J_{Pt-H}$ = 62.8 Hz; 1H, Pt−*CH*MePh), 1.17 (d; ^3J = 6.6 Hz; 3H, Pt−η^3-CH*Me*Ph). ^{13}C{^{1}H} NMR (100 MHz, CD_2Cl_2): key chemical shifts for the major isomer, 78.07 (satellite; $^2J_{Pt-C}$ = 93 Hz; ortho Pt−η^3-CHMe*Ph*), 43.67 (satellite; $^2J_{Pt-C}$ = 284 Hz; Pt−η^3-*CH*MePh), 15.74 (satellite; $^3J_{Pt-C}$ = 200

Table 1. Crystallographic Data for Compounds 3−5

	3	4	5
formula	$C_{62}H_{38}N_5B$-$F_{24}Pt$	$C_{57}H_{36}N_5F_{24}$-BPt	$C_{64}H_{40}N_4F_{24}$-BPt
fw	1514.87	1452.8	1526.90
space group	$P\bar{1}$	$P\bar{1}$	$P\bar{1}$
a, Å	12.698(4)	12.4783(12)	16.4420(17)
b, Å	13.177(5)	13.0894(12)	18.7653(19)
c, Å	19.064(6)	18.1842(18)	21.650(2)
α, deg	90.973(7)	79.260(2)	65.647(2)
β, deg	93.076(7)	76.753(2)	85.831(2)
γ, deg	95.273(6)	86.854(2)	89.751(2)
V, Å^3	3171.1(18)	2840.2(5)	6067.1(11)
Z	2	2	4
d_{calcd}, g cm^{-3}	1.587	1.699	1.672
μ, cm^{-1}	23.26	25.93	24.32
$2\theta_{max}$, deg	56.76	56.64	56.74
no. of rflns measd	19 248	20 140	43 522
no. of rflns used	12 918	12 910	27 602
R_{int}	0.0814	0.0416	0.0644
no. of params	1028	822	1459
final *R* ($I > 2\sigma(I)$)			
R1[a]	0.0761	0.0959	0.0770
wR2[b]	0.1392	0.2318	0.1370
R (all data)			
R1[a]	0.2510	0.1975	0.2342
wR2[b]	0.1897	0.2668	0.1612
GOF on F^2	0.916	0.955	0.718

[a] $R1 = \sum||F_o| - |F_c||/\sum|F_o|$. [b] $wR2 = [\sum w[(F_o^2 - F_c^2)^2]/\sum[w(F_o^2)^2]]^{1/2}$; $w = 1/[\sigma^2(F_o^2) + (0.075P)^2]$, where $P = [\mathrm{Max}(F_o^2,0) + 2F_c^2]/3$.

Hz; Pt−η^3-CH*Me*Ph); key chemical shifts for the minor isomer, 75.43 (satellite; $^2J_{Pt-C}$ = 86 Hz; ortho Pt−η^3-CHMe*Ph*), 38.62 (satellite; $^2J_{Pt-C}$ = 280 Hz; Pt−η^3-*CH*MePh), 14.12 (satellite; $^3J_{Pt-C}$ = 199 Hz; Pt−η^3-CH*Me*Ph).

Conversion of the η^3 Complex 5 to the η^1-Benzylic Complex 3. A 15 mg portion of the η^3 complex **5** (∼1 × 10^{-5} mol) was placed in a NMR tube, and CD_2Cl_2 (0.5 mL) was added to dissolve the sample at ambient temperature. After a ^{1}H NMR spectrum was recorded, CD_3CN (17 μL, ∼3 × 10^{-4} mol) was added to the NMR tube, and a series of ^{1}H NMR spectra were recorded every 5 min at ambient temperature. No conversion was detected at temperatures below −10 °C. The conversion at room temperature was fairly slow, despite the excess amount of CD_3CN used. The ^{1}H NMR spectra indicated that after ∼1 h the η^3 compound was nearly completely converted to the η^1-benzylic C product **3**. Notably, the ratio of the two sets of signals for the diastereomers of **3** after the conversion was about the same as that of the two isomers of the η^3 complex **5**.

The conversion of complex **6** to complex **4** was carried out in the same manner by using compound **6**. NMR experiments showed that compound **6** can also react with acetonitrile at ambient temperature to afford the η^1-benzylic C−H activation product **4** quantitatively.

X-ray Diffraction Analysis. Single crystals of **3** were obtained from recrystallization of the crude product with THF/hexanes. Single crystals of **4** were obtained from the reaction mixture after the slow evaporation of the solvent. Single crystals of **5** were obtained from the reaction mixture after being kept for several weeks in the refrigerator. Crystals were mounted on glass fibers for data collection. Data were collected on a Siemens P4 single-crystal X-ray diffractometer with a Smart CCD-1000 detector and graphite-monochromated Mo Kα radiation, operating at 50 kV and 35 mA at 298 K for **3** and at 180 K for **4** and **5**, respectively. No significant decay was observed for all of the samples. Data were processed on a PC using the Bruker SHELXTL software package[14] (version 5.10) and were corrected for Lorentz and polarization effects. Crystals of **3**−**5** all belong to the triclinic space group $P\bar{1}$.

(14) SHELXTL NT Crystal Structure Analysis Package, Version 5.10; Bruker AXS, Madison, WI, 1999.

Table 2. Selected Bond Lengths (Å) and Angles (deg) for 3A, 4A, and 5

Compound **3A**			
Pt(1)−N(5)	1.883(15)	Pt(1)−C(27)	2.025(17)
Pt(1)−N(1)	1.932(11)	Pt(1)−N(3)	2.153(10)
N(5)−Pt(1)−N(1)	179.2(5)	N(5)−Pt(1)−N(3)	92.3(4)
N(5)−Pt(1)−C(27)	89.9(7)	N(1)−Pt(1)−N(3)	87.1(4)
N(1)−Pt(1)−C(27)	90.8(7)	C(27)−Pt(1)−N(3)	169.7(7)
Compound **4A**			
Pt(1)−N(5)	1.984(13)	Pt(1)−C(19)	2.070(11)
Pt(1)−N(3)	2.033(12)	Pt(1)−N(1)	2.145(8)
N(5)−Pt(1)−N(3)	178.9(4)	N(5)−Pt(1)−N(1)	89.2(4)
N(5)−Pt(1)−C(19)	90.0(6)	N(3)−Pt(1)−N(1)	91.7(3)
N(3)−Pt(1)−C(19)	89.1(6)	C(19)−Pt(1)−N(1)	178.5(7)
Compound **5**			
Pt(1)−N(1)	2.071(11)	Pt(2)−N(5)	2.067(10)
Pt(1)−C(23)	2.124(11)	Pt(2)−N(7)	2.094(8)
Pt(1)−N(4)	2.137(8)	Pt(2)−C(52)	2.110(12)
Pt(1)−C(28)	2.213(14)	Pt(2)−C(50)	2.118(11)
Pt(1)−C(22)	2.304(16)	Pt(2)−C(51)	2.145(11)
N(1)−Pt(1)−C(23)	134.4(4)	N(5)−Pt(2)−N(7)	86.0(3)
N(1)−Pt(1)−N(4)	86.6(3)	N(5)−Pt(2)−C(52)	169.6(4)
C(23)−Pt(1)−N(4)	134.7(4)	N(7)−Pt(2)−C(52)	103.9(4)
N(1)−Pt(1)−C(28)	104.4(5)	N(5)−Pt(2)−C(50)	100.0(5)
C(23)−Pt(1)−C(28)	37.9(4)	N(7)−Pt(2)−C(50)	173.9(4)
N(1)−Pt(1)−C(22)	172.1(5)	C(52)−Pt(2)−C(50)	70.1(5)
C(23)−Pt(1)−C(22)	40.6(4)	N(5)−Pt(2)−C(51)	133.6(5)
N(4)−Pt(1)−C(22)	100.6(4)	N(7)−Pt(2)−C(51)	134.7(5)
C(28)−Pt(1)−C(22)	68.2(5)	C(52)−Pt(2)−C(51)	39.2(4)
N(4)−Pt(1)−C(28)	167.9(4)	C(50)−Pt(2)−C(51)	39.7(4)

Chart 2

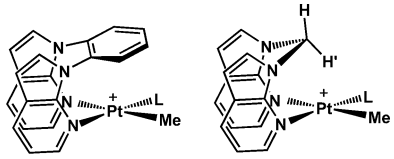

There are two independent molecules of **5** in the unit cell. Disordered ethylbenzene solvent molecules were located in the lattice of **5** and refined successfully. The phenyl group in **4** displays a rotational disordering. Two sets of phenyl atoms with 50% occupancy for each site were located and refined successfully. Most of the non-hydrogen atoms were refined anisotropically. Most of the CF_3 groups in **3**−**5** display rotational disorders, which were modeled and refined successfully. The positions of hydrogen atoms were calculated, and their contributions in structure factor calculations were included. The crystal data for **3**−**5** are listed in Table 1. Important bond lengths and angles are given in Table 2.

Results and Discussion

Ethylbenzene C−H Bond Activation using Complexes 1 and 2. (a) Regioselectivity. As reported earlier[12] in the benzene and toluene activation reactions, the Pt(II) complexes **1** and **2** are precursor compounds that can be used for C−H bond activation after the in situ generation of the cationic species shown in Chart 2 (where L is a solvent molecule or Et_2O) by the addition of an acid.

The electronic impacts of the BAB and the BAM ligands on the Pt center appear to be similar, as evidenced by the CO stretching frequencies of the CO complexes [Pt(BAB)Me(CO)]-[BAr′$_4$] (2106 cm^{-1}) and [Pt(BAM)Me(CO)][BAr′$_4$] (2119 cm^{-1}) (see the Supporting Information).

The addition of the acid to the suspension of **1** in dry ethylbenzene at ambient temperature resulted in the immediate

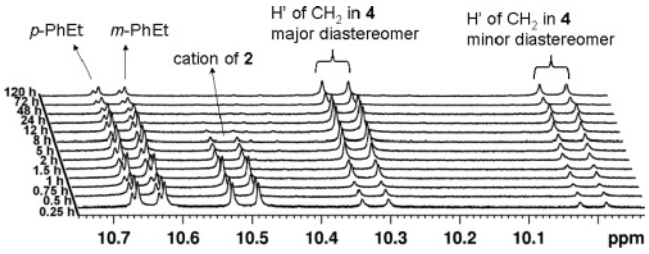

Figure 1. ^{1}H NMR spectra of the low-field region of the reaction mixture of ethylbenzene C−H activation by the cation of **2**, showing the distribution change of aryl C−H activation products (*p*- and *m*-Ph) versus the benzylic product **4** with time.

formation of a clear pink solution. To examine the kinetic and thermodynamic selectivity, the reaction mixture was sampled at various time intervals and subjected to ^{1}H NMR spectroscopic analyses after treatment with acetonitrile. Consistent with our previous observation for toluene C−H activation,[12a] the aromatic C−H activation products were again found to be the dominant species (meta and para) at the early stage of the reaction, which were converted to the benzylic product with time; this product was isolated as [Pt(BAB)(CH_3CN)(CH(Me)Ph)][BAr'_4] (**3**), whereas no *o*-aryl product was observed during the whole process. Therefore, the benzylic activation is a thermodynamically preferred process while the aromatic activation is kinetically favored. This is in good agreement with the recent reports by Bercaw and co-workers.[6j,k] After 5 days, the cationic starting material was completely consumed and the ratio between the benzylic C−H activation product and aryl C−H activation products (meta and para) was >9:1.

The ethylbenzene C−H activation with complex **2** was investigated using a similar procedure. To facilitate the ^{1}H NMR spectral assignments of the products, the para aromatic C−H activation product [Pt(BAM)(*p*-Ph-Et)(CH_3CN)][BAr'_4] (see the Supporting Information) was synthesized. Not surprisingly, the ^{1}H NMR spectroscopic analyses of the reaction mixture revealed that the para and meta aromatic C−H activation products were once again kinetically preferred. The spectrum recorded after 15 min showed a mixture of products consisting of para and meta aromatic products (50%), benzylic product (**4**, 18%), and the cationic starting material (32%). After 3 days, the starting material was completely consumed, as shown by the stacked ^{1}H NMR spectra of the reaction mixture in the distinct low-field region recorded over a 5-day period (Figure 1). The product distribution between the benzylic C−H activation and aromatic C−H activation after 5 days was ∼3.7:1, an indication that compound **2** has a lower regioselectivity, compared to compound **1**. Considering their similar electronic properties, this regioselectivity difference between **1** and **2** toward ethylbenzene C−H activation can be attributed to the steric difference between the BAB and the BAM ligands—the former is apparently more sterically demanding than the latter, as shown by the crystal structures of **1** and **2** in Figure 2. The complex [Pt(BAM)(CH_3CN)(CH(Me)Ph)][BAr'_4] (**4**) was isolated and fully characterized by NMR, elemental, and single-crystal X-ray diffraction analyses.

(b) Diastereoselectivity. Because of the asymmetric blocking on one side of the Pt(II) coordination plane by the BAB and BAM ligands in **1** and **2**, respectively, the cationic species shown in Chart 2 have a chiral structure (with both enantiomers being present). Unlike toluene which, after the cleavage of a C−H bond on the methyl group, does not produce any chiral center, the cleavage of a C−H bond on the CH_2 group of the ethylbenzene molecule leads to the formation of a chiral center.

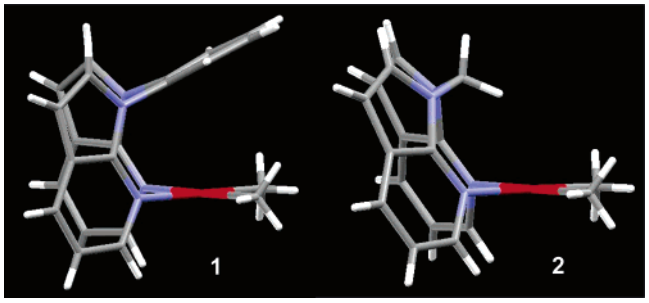

Figure 2. Side view of the structures of **1** and **2** showing the blocking of the linker to the Pt center.

Chart 3

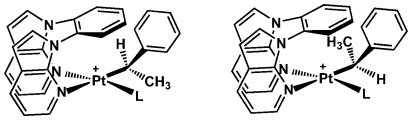

Sketch 3

The coexistence of the two chiral centers (one Pt-based and one carbon-based) in the cationic complexes of **3** and **4**, in principle, should result in the formation of two diastereomers (*RR* and *RS* or their enantiomers *SS* and *SR*) for each complex, as illustrated by the structures **3A** and **3B** of the cation of **3** in Chart 3 (the diastereomers **4A** and **4B** for the cation of **4** have similar structures and, hence, are not shown). The key aspect of our investigation was therefore to determine if the ethylbenzene C−H activation by the Pt(II) complexes **1** and **2** has any preference for one diastereomer over the other: i.e., diastereoselectivity.

Crystal Structures of [Pt(BAB)(CH_3CN)(CH(Me)Ph)][BAr'_4] (3A) and [Pt(BAM)(CH_3CN)(CH(Me)Ph)][BAr'_4] (4A). The structures of the cationic portions of **3** and **4** are shown in Figure 3. The basic structural features of **3** resemble those of the toluene analogue[12a] [Pt(BAB)(CH_3CN)(CH_2Ph)]$^+$ reported earlier by us. The BAB and the BAM ligands have orientations similar to those observed in the starting materials **1** and **2**. The shortest contact distance between the carbon atoms of the BAB phenyl ring and the Pt center in **3** is 3.16 Å, while the contact distance between one of the protons of the BAM CH_2 and the Pt center in **4** is 2.46 Å (the contact distance between the CH_2 carbon atom and the Pt center is 3.16 Å). There are two important key features for these two compounds, as revealed by the structures. First, the phenyl group of the activated ethylbenzene is oriented "up" toward the chelate ligand BAB in **3** and BAM in **4**, despite the obvious steric congestion in this orientation. We have observed the same phenomena in the crystal structures of [Pt(BAB)(L)(CH_2Ph)]$^+$, where L = CH_3CN, SMe_2. One possible explanation for this unexpected orientation of the phenyl group is the attraction between the aromatic phenyl ring and the aromatic 7-azaindolyl rings of the chelate ligands. The second important feature is that the diastereomers of the two crystal structures have an identical stereogeometry, which corresponds to the diastereomer **3A** (or **4A**) or its enantiomer shown in Chart 3. The chiral carbon centers in the structures **3A** and **4A**, as shown in Figure 3, have the same *S* chirality (the inversion-center-related enantiomers coexist in the crystal lattice for both compounds). To determine if the stereogeometry revealed by the crystal structures represents the major diastereomer for both compounds in solution, we investigated the reaction mixture by NMR spectroscopic methods.

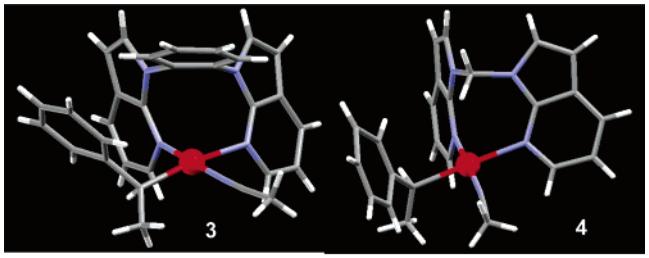

Figure 3. Crystal structures of the η^1-benzylic complexes **3A** and **4A**. Thermal ellipsoid drawings with labeling schemes can be found in the Supporting Information.

Diastereomer Distribution in the Reaction Mixture. Due to the significant difference between the structures **3A** and **3B** (or **4A** and **4B**), it was anticipated that these two diastereomers may display distinct chemical shifts in NMR spectra. Indeed, two distinct sets of chemical shifts corresponding to the two diastereomers for the CH and the CH_3 protons of the −CH(Me)Ph group were observed in the ^{1}H NMR spectrum of the isolated complex **3** and the spectrum of the reaction mixture of the cation of **1** with ethylbenzene, as shown by Figure 4 (the full spectrum is provided in the Supporting Information). The protons of the CH and the CH_3 groups display characteristic ^{195}Pt−H coupling satellites with fairly large ^2J and ^3J ^{195}Pt−H coupling constants (∼104 and ∼50 Hz, respectively). Most importantly, as shown in Figure 4, the intensities of the two sets of signals are not equal, with a ratio of ∼3.7:1.0 in the final reaction mixture. The NMR data unambiguously established that the ethylbenzene C−H bond activation by complex **1** proceeds not only regioselectively but also diastereoselectively. It is noteworthy that a similar diastereoselectivity of such an intermolecular process has not been reported in previously known cationic Pt(II) systems.

Similarly, the reaction mixture of the cation of **2** with ethylbenzene after the termination by acetonitrile and the isolated product **4** also displays two distinct sets of chemical shifts that correspond to the two diastereomers **4A** and **4B** in the ^{1}H NMR spectra (see the Supporting Information). For the CH and the CH_3 protons, characteristic ^{195}Pt−H coupling satellites were once again observed, with ^{195}Pt−H ^2J and ^3J coupling constants being ∼110 and ∼40 Hz, respectively. However, as shown by Figure 4, the observed ratio of the two diastereomers for **4** is ∼1.5:1.0, much lower than that of **3**. Thus, the BAM Pt system displays not only a relatively low regioselectivity but also a relatively low diastereoselectivity in ethylbenzene C−H activation, compared to the case for the BAB Pt system. Again, the obviously more effective blocking group, phenyl, in the BAB ligand, compared to the CH_2 group in the BAM ligand, appears to be responsible for the observed difference in diastereoselectivity between these two systems.

Structures of 3 and 4 in Solution. To determine the molecular structures of compounds **3** and **4** in solution, we used 2D ^{1}H NOESY NMR spectroscopy. Figure 5 shows portions of the NOESY spectrum for compound **3** in CD_2Cl_2 solution (the complete 2D NOESY spectra for **3** and **4** are provided in the Supporting Information). As expected, strong cross-peaks are observed between CH_3, CH, and the ortho protons from the phenyl group for both diastereomers **A** and **B**. The most direct NMR evidence revealing the absolute configuration comes from NOE cross-peaks between CH_3, CH, and H6 of the 7-azaindolyl ring. As seen from Figure 5, for the **A** diastereomer the CH−H6 cross-peak is considerably stronger than the CH_3−H6 cross-

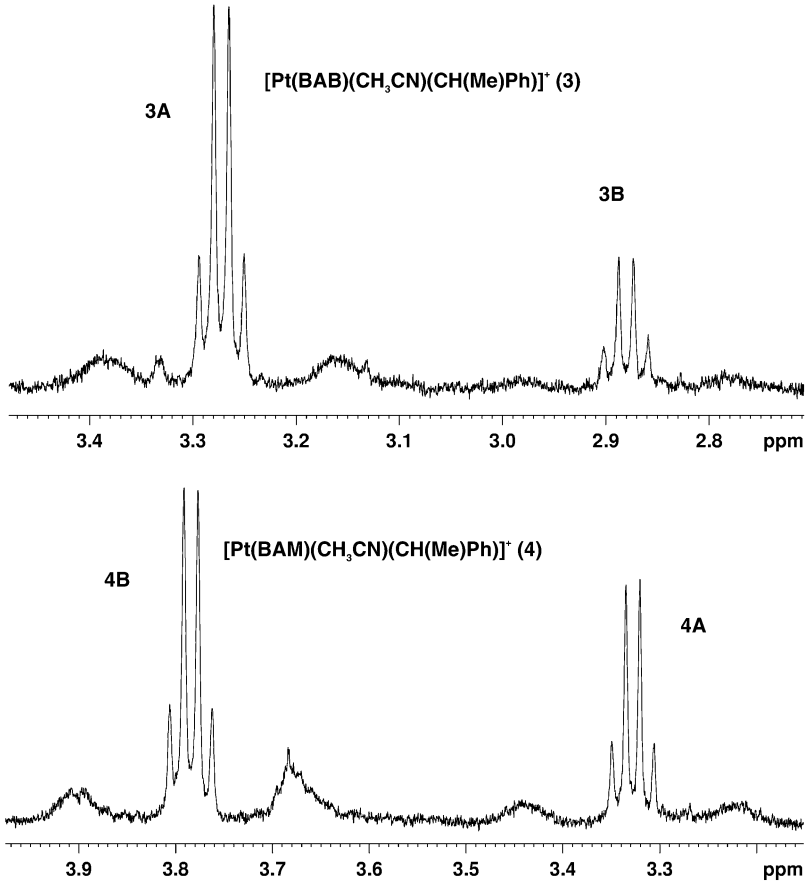

Figure 4. ^{1}H NMR spectra in CD_2Cl_2 showing the chemical shifts and the relative intensity of the C*H*(Me) proton of the two diastereomers in **3** and **4** in the reaction mixtures.

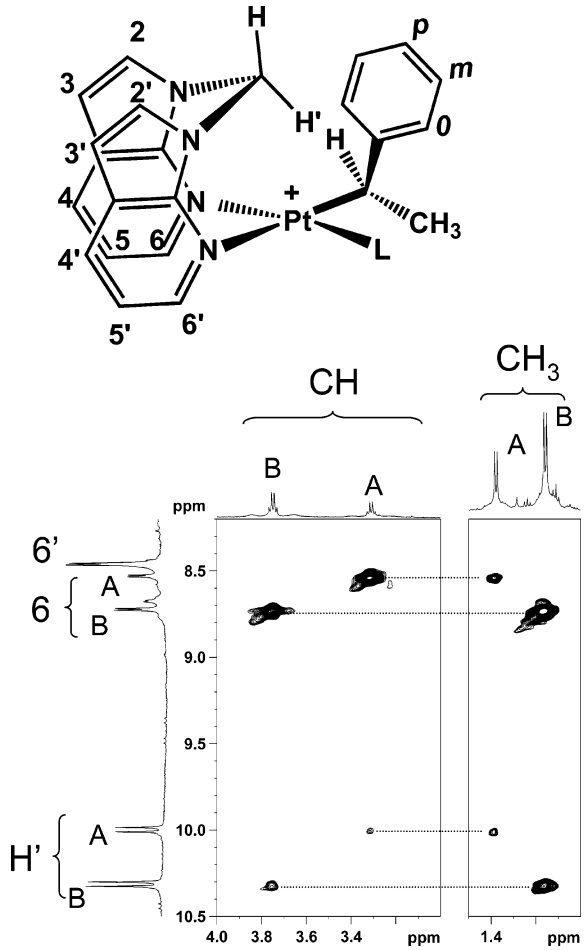

Figure 5. Portions of the 2D ^{1}H NOESY spectrum for compound **4** in CD_2Cl_2 at 298 K obtained on a Bruker Avance-600 NMR spectrometer (B_0 = 14.1 T). A mixing time of 400 ms was used. Two transients were collected for each of the 512 t_1 increments with a recycle delay of 2 s. The structure shown is diastereomer **A**.

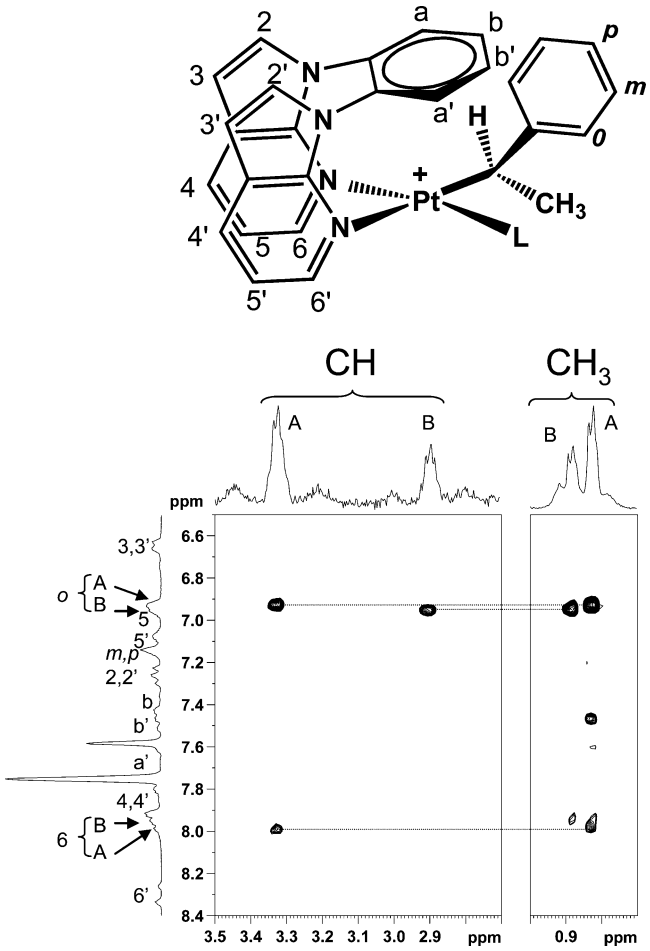

Figure 6. Portions of the 2D ^{1}H NOESY spectrum for compound **3** in CD_2Cl_2 at 298 K. A mixing time of 400 ms was used. The structure shown is diastereomer **A**.

peak, indicating that the CH group is pointing toward H6: i.e., the 7-azaindolyl ring. In contrast, the two corresponding cross-peaks for the **B** diastereomer have similar intensities. It is also important to note that the CH_3−H6 cross-peak for **B** is much greater than the corresponding CH_3−H6 cross-peak for **A**, which cannot be accounted for simply by the population difference between the two methyl peaks. This is further proof that the CH_3 in the diastereomer **B** is much closer to H6 of the 7-azaindolyl ring than the CH_3 in the diastereomer **A**. Another interesting question is whether the phenyl ring of the CH(Me)-Ph group in both isomers maintains the same orientation with respect to the 7-azaindolyl ring ligands. Strong NOE cross-peaks are observed between the ortho protons and H′ of the CH_2 bridge (but no cross-peaks were observed between the ortho protons and the other proton in the same CH_2 group, H) for both isomers, an indication that the phenyl ring is oriented toward the CH_2 bridge in the same manner as shown by the crystal structure. Further, the cross-peak intensities are consistent with the population ratio between the **A** and **B** diastereomers. This suggests that the phenyl groups of the **A** and **B** diastereomers have approximately the same distance (but not necessarily the same orientation) to the CH_2 bridge. The observed CH−H′ and CH_3−H′ cross-peaks shown in Figure 5 also confirm that the absolute configuration of the major diastereomer of **4** in solution is **4B**, opposite to that observed in the crystal structure.

In contrast to the case for **4**, the same NOESY spectral analysis established that the major diastereomer for **3** has the structure **3A**, which has the same stereogeometry as the crystal structure. The most important evidence supporting this assignment is the strong CH−H6 cross-peak for isomer **A**, as shown in Figure 6, which is absent for isomer **B**, supporting that the CH proton of the benzylic group in **A** is closer to the 7-azaindolyl ring than that of **B**. In addition, a strong CH_3−Hb (Hb′) cross-peak was also observed for isomer **A**, but not isomer **B**, which is again consistent with the diastereomer **3A** being the major isomer. For the complete 2D NOESY NMR spectra, please see the Supporting Information.

The preference for the diastereoisomer **A** by compound **3** may be explained by the fact that, in **3A**, the unfavorable interactions between the methyl group and the 7-azaindolyl ring are minimized. However, the same rationale clearly does not apply for the relatively high selectivity for isomer **B** by **4**, since **B** has a chirality on the carbon center which is opposite to that in **A**. To understand the origin of the contrasting diastereoselectivity by **3** and **4**, efforts were made to analyze and isolate the possible intermediates involved in the formation of **3** and **4**.

Isolation and Characterization of the η^3 Complexes [Pt(BAB)(η^3-CHPh(Me))][BAr′$_4$] (5) and [Pt(BAM)(η^3-CHPh(Me))][BAr′$_4$] (6). In order to identify the reaction intermediates, ideally the reaction mixture should be monitored using solvents that do not introduce any coordinating ligand such as acetonitrile. Due to the highly reactive nature of the starting materials **1** and **2** toward halogenated solvents, conventional NMR solvents such as CD_2Cl_2 cannot be used to monitor the reaction. We

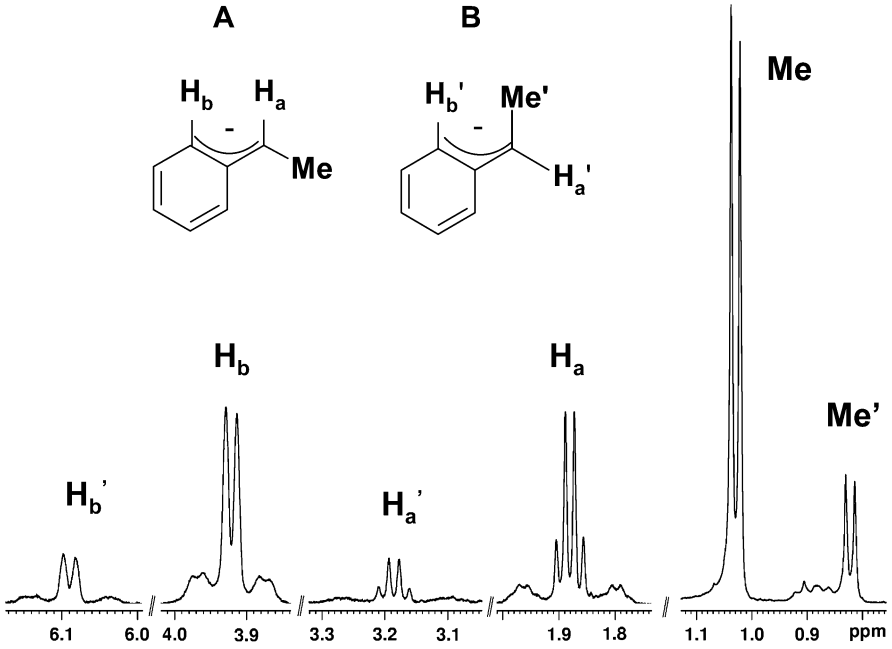

Figure 7. ^{1}H NMR spectra of the η^3-ethylbenzene group in **5** in CD_2Cl_2 showing the chemical shifts and the proposed structures of the two isomers.

also tried to use CF_3CD_2OD as a NMR solvent to follow the reaction. However, this solvent generated complicated species in the reaction and interfered with the reaction. As a result, direct monitoring of the ethylbenzene C−H bond activation process using compound **1** or **2** by NMR could not be achieved. Since the NMR data for the acetonitrile-terminated reaction showed that after about 5 days all starting materials were consumed and the reaction mixture did not change further with time, we decided to investigate the 5 day reaction mixture without the addition of acetonitrile. The 5 day reaction mixtures of **1** and **2** with $[(Et_2O)_2H][BAr'_4]$ and ethylbenzene were examined by ^{1}H and ^{13}C NMR in CD_2Cl_2. For the ethylbenzene reaction with **1**, the ^{1}H NMR data indicated that, in addition to the presence of a small amount of aryl C−H activation products, the η^3-benzylic compound was the major product. No η^1-benzylic compound was observed. In addition, it appeared that there were two types of η^3-benzylic species in the reaction mixture with a ratio of ~3.7:1. To fully characterize the elusive η^3 compound, we tried to isolate the η^3-benzylic compound from the reaction mixture and our efforts were successful. The η^3 compound **5** was obtained as a crystalline solid in about 70% yield. The ^{1}H NMR and ^{13}C NMR spectra for the isolated solid **5** also showed two sets of well-resolved chemical shifts of two distinct η^3 compounds with an intensity ratio similar to that of the reaction mixture, as shown in Figure 7. The diagnostic signals for the η^3-benzylic group are the ortho proton of the phenyl group (δ 3.92 and 6.09 ppm, respectively, for the two isomers) and the proton of the C*H*(Me) group (δ 1.88 and 3.18 ppm, respectively, for the two isomers), both of which display characteristic ^{195}Pt−H coupling with a coupling constant of ~40 and ~67 Hz, respectively. In the ^{13}C NMR spectrum, two sets of chemical shifts for the ortho carbon of the phenyl group and the C*H*(Me) carbon atom with distinct ^{195}Pt−^{13}C coupling satellites were also observed. On the basis of the NMR pattern, the formula of $[Pt(BAB)(\eta^3\text{-}CH(Me)Ph)][BAr'_4]$ was proposed for **5**.

To understand the origin of the two different η^3 species of **5**, we determined the crystal structure of **5** by a single-crystal X-ray diffraction analysis. The structure of the cation in **5** is shown in Figure 8 (there are two independent molecules of **5** in the asymmetric unit with identical structures). Again, the structure

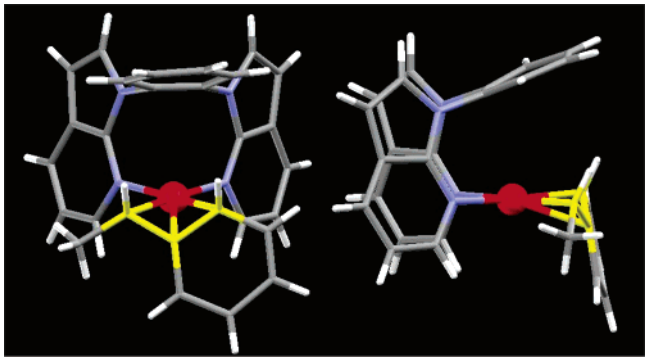

Figure 8. Crystal structure of the cation of **5** with two different views. The detail of this structure with labeling schemes is provided in the Supporting Information.

of the cation **5** has no symmetry, but both enantiomers coexist in solution and in the crystal lattice. The CH(Me)Ph group in **5** is bound to the Pt center sideways through three carbon atoms, the η^3 fashion typically observed for an allyl group. The bond lengths from the Pt center to the three carbon atoms are similar. Although η^3-type allyl Pt(II) complexes are well-known,[8c,f] the structure of **5** is the first direct structural proof of the η^3-benzylic Pt(II) complexes proposed by Bercaw et al. On the basis of the crystal structure of **5**, the two types of η^3 compounds observed in the NMR spectra can be attributed to the coexistence of two structural isomers, as depicted in Figure 7 and Scheme 1. In the major isomer the CH proton and the ortho proton of the phenyl ring are on the same side, as shown by the crystal structure, while in the minor isomer, the CH_3 group is on the same side with the ortho proton. As shown by the crystal structure, for the BAB compound, there is little space between the phenyl group of the BAB ligand and the η^3-benzylic ligand. As a consequence, the interligand steric interactions in the minor isomer are much greater than those in the major isomer, thus leading to the preferential formation of the major isomer for **5**. NMR data analyses established that the major isomer of **5** has the same structure as the crystal structure.

The NMR spectra for the 5 day reaction mixture of the BAM complex **2** with $[(Et_2O)_2H][BAr'_4]$ and ethylbenzene in the

Scheme 1. Stereospecific Conversion of 5 to 3

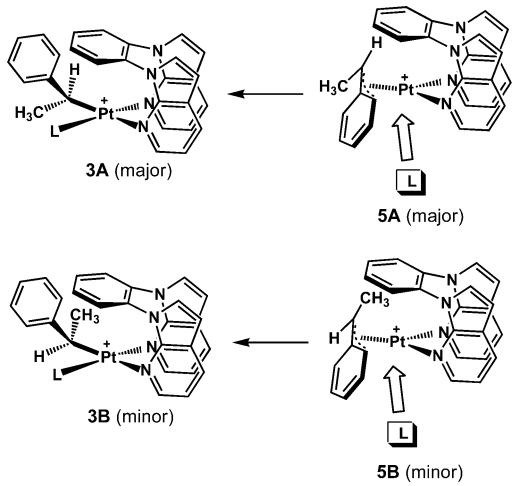

absence of donor solvents also displayed two distinct sets of chemical shifts for the η^3-benzylic products with a ratio of ~1.5:1, attributable to the two η^3 isomers (Figure 9). Although we have not been able to isolate the η^3-benzylic product [Pt(BAM)-(η^3-CHPh(Me))][BAr′$_4$] (**6**) as a pure crystalline compound, the two η^3 isomers of **6** are believed to have the same structures as those of **5**. The diminished ratio of the major isomer versus the minor isomer of **6**, compared to that of **5**, is evidently caused by the diminished steric congestion in **6**. To establish that the major isomer of **6** indeed has the same structure as the major isomer **A** of **5**, 2D NOESY NMR experiments were performed for compound **6** in CD_2Cl_2 and portions of the spectrum are shown in Figure 9 (the complete 1D spectrum and 2D NOESY spectrum for **6** are provided in the Supporting Information). Unexpectedly, however, the methyl group of the major isomer shows a strong cross-peak with the H′ proton of the CH_2 bridge, while the same cross-peak is absent for the minor isomer. This is a strong indication that the major isomer of **6** has the structure **B**, as depicted in Figures 7 and 9, instead of **A**. Consistent with this assignment is the weak cross-peak between Ha and H′ for the minor isomer, as shown in Figure 9. At first glance, this seems counterintuitive, since isomer **B** appears to be more sterically congested than **A** does. The 2D NOESY NMR data, in fact, provided a clue for this puzzle. As shown in Figure 9, the methyl group of the minor isomer has a very large cross-peak with H6 of the 7-azaindolyl ring, an indication that in isomer **A** the methyl group is considerably close to the 7-azaindolyl ring, generating a sterically crowded environment, which we reasoned results in a smaller population of the isomer **A**. As shown by the bond distance and angle data in Table 2, the N−Pt−N chelate angle for BAB complexes (86−87°) is in general much smaller than that of the BAM complex (92°), which means that the methyl group and the 7-azaindolyl ring in **6A** would be much closer and, thus, have stronger interactions than those in **5A**. Although in isomer **6B** the interaction between the methyl group and the CH_2 group is greater than that in **6A**, it is lessened to a great extent due to the incomplete blocking of the fifth Pt coordination site by the CH_2 bridge, compared to the case for **5B**, where the phenyl bridge completely blocks the fifth Pt coordination site, causing a much stronger interaction

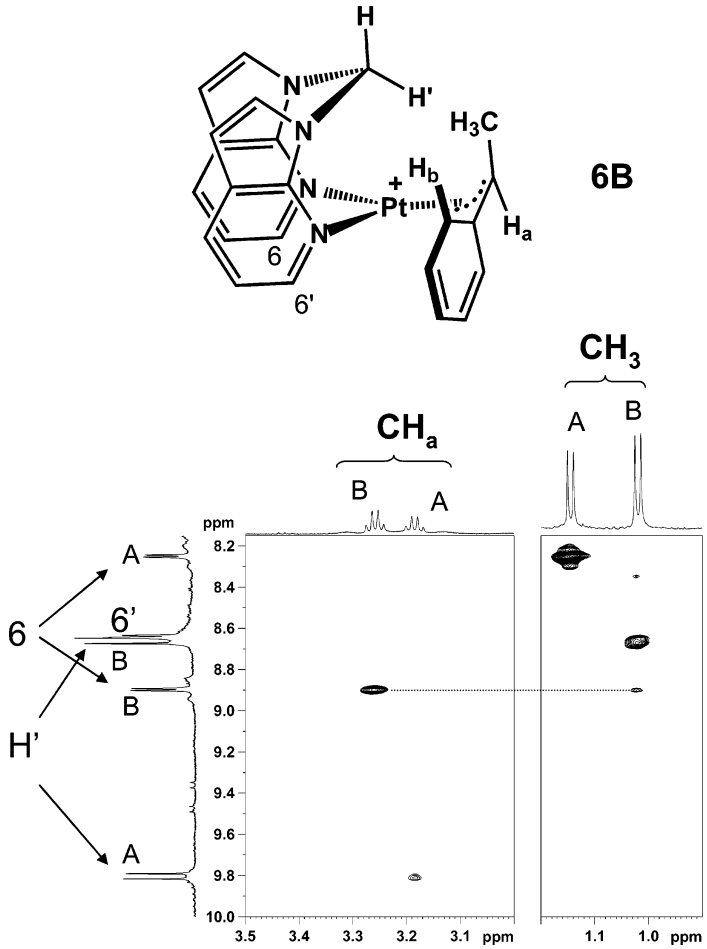

Figure 9. Portions of the 2D ^{1}H NOESY spectrum for compound **6** in CD_2Cl_2 at 298 K. A mixing time of 400 ms was used. The structure shown is the major isomer **6B**.

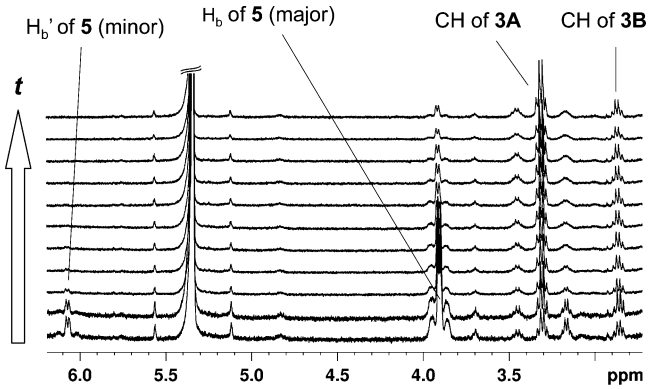

Figure 10. ^{1}H NMR spectra in the 2.7−6.2 ppm region showing the conversion of the isomers of the η^3 complex **5** to the diastereomers of the η^1 complex **3** with the retention of the isomer ratio after the addition of excess CD_3CN (∼30-fold). The spectra were recorded at ambient temperature at 5 min intervals in CD_2Cl_2.

between the CH_3 and the phenyl group. The greater population of isomer **6B** over **6A** is therefore the consequence of tradeoff between a methyl−CH_2 interaction versus a methyl−7-azaindolyl interaction. The contrasting selectivities for different η^3 isomers by **5** and **6** again demonstrate the subtle impact of the steric blockage imposed by the BAB and BAM ligands.

Conversion of the η^3-Benzylic Compounds to the η^1-Benzylic Compounds. One key observation in characterizing the η^3 compounds was that the isomer ratios for the η^3 compounds **5** and **6** are approximately the same as those of the diastereoisomers of the η^1-benzylic compounds **3** and **4**, which caused us to consider that the η^3-benzylic compounds are likely precursors to the η^1-benzylic product. To confirm that the η^3 compound can indeed be converted to the η^1 compound, we monitored the reaction of the isolated η^3 compound **5** (a mixture of both isomers) with CD_3CN by ^{1}H NMR spectra in CD_2Cl_2. Indeed, as shown by the NMR spectra in Figure 10, compound **5** was converted quantitatively to the η^1 compound **3** and the resultant diastereomer ratio of **3** was the same as the isomer ratio of the η^3 compound **5**. This conversion is not surprising, since similar η^3 to η^1 conversion was observed by Bercaw and co-workers.[6k,j] The significance of this experiment lies in the fact that it established a direct link between the major η^3 isomer of **5A** and the major diastereomer of **3A** and that between the minor η^3 isomer of **5B** and the minor diastereomer **3B**. Similar experiments on the addition of acetonitrile to the η^3 isomer mixture of **6** confirmed the same specific transformation to the η^1 compound **4** with the retention of the isomer ratios. We believe that this specific transformation of one η^3 isomer of **5** or **6** to one η^1 diastereomer of **3** or **4** is a manifestation/consequence of the asymmetric blocking of the Pt(II) coordination plane by the BAB or BAM ligand. As shown by Scheme 1, the blocking of the Pt(II) center by the chelate ligand forces the acetonitrile ligand to approach the Pt(II) center from the bottom, replacing the π-bound phenyl group, resulting in the diastereoselective formation of the η^1-benzylic complex. The exclusive formation of the major diastereomer **3A** with *S* chirality on the CH center from the major η^3 isomer and of the minor diastereomer **3B** with the *R* chirality on the CH center from the minor η^3 isomer are illustrated in Scheme 1. It has been shown by Bercaw and co-workers that in the absence of donor ligands such as acetonitrile, certain cationic η^1-benzylic complexes can be converted to the η^3 complexes via either inter- or intramolecular processes.[6j] To determine if this pathway is also operative in our system, we synthesized [Pt(BAM)(η^1-CH_2-Ph)$_2$] (see the Supporting Information) and monitored the solution of the cation [Pt(BAM)(η^1-CH_2Ph)(solvent)]$^+$ generated in situ by the addition of 1 equiv of $[(Et_2O)_2H][BAr'_4]$ using solvents such as acetone-d_6 and C_6F_6 by ^{1}H NMR. Although a trace amount of the η^3-CH_2Ph compound appeared to be present, >90% of the compound was an η^1-CH_2Ph complex (stabilized by acetone or adventitious water). On the basis of these observations, we suggest that the η^3 complexes **5** and **6** are the most likely intermediates in the formation of the η^1-benzylic complexes **3** and **4** from the ethylbenzene reactions with the BAB complex **1** and the BAM complex **2**, respectively. We further suggest that the diastereoselectivity displayed by **3** and **4** is dictated by the asymmetric structure of the η^3 precursor, which is the direct consequence of the asymmetric blocking of the Pt center by the BAB or BAM ligand.

Conclusions

The BAB and BAM Pt(II) complexes activate alkyl-substituted benzene readily. The η^1-benzylic C−H activation products are thermodynamically favored for both complexes, with the BAB complex displaying a greater regioselectivity toward the benzylic product than the BAM complex. Most importantly, both BAB and BAM complexes display diastereoselectivity for the η^1-benzylic C−H activation products. Once again, the Pt BAB complex has a higher diastereoselectivity (3.7:1) than the BAM complex (1.5:1). However, the BAB and the BAM complexes display different preferences for the diastereomer. NMR analyses established that the dominating diastereomer in solution is **3A** for **3** and **4B** for **4**, respectively.

The isolation and characterization of the η^3-benzylic complexes **5** and **6**, the identification of the two structural isomers with a nonequal distribution, and the demonstration of their stereospecific conversion to the corresponding η^1-benzylic compounds in the presence of a donor such as CH_3CN, along with the fact that the isomer ratio of the η^3-benzylic complex in the reaction mixture for both BAB and BAM complexes is about the same as that of the diastereomer ratio of the η^1-benzylic products in the reaction mixture terminated by CH_3CN cause us to suggest the following. (1) The η^3-benzylic complex is mostly likely a reaction intermediate or a precursor compound to the η^1-benzylic complex. (2) The apparent diastereoselectivity displayed by the BAB and BAM complexes in the formation of the η^1-benzylic complex is due to the selective formation and the asymmetric structures of the two η^3-benzylic isomers. (3) The preferential formation of one η^3 isomer over the other by the BAB and BAB complexes is the consequence of the asymmetric blocking of the Pt axial coordination sites by the chelate ligand. (4) The contrasting preference for the dominating η^3-benzylic isomer by the BAB complex (favoring isomer **A**) and the BAM complex (favoring isomer **B**) is most likely caused by the difference in steric blocking by the phenyl bridge in BAB and the CH_2 bridge in BAM and the N−Pt−N chelate angle in the two complexes.

In summary, this work demonstrates the importance of the steric geometry and the blocking effect of the N,N chelate ligands in diastereoselective ethylbenzene C−H bond activation by cationic Pt(II) complexes and provides new insight into the key role played by the η^3-benzylic complex.

Acknowledgment. We thank the Natural Sciences and Engineering Research Council of Canada for financial support of this work.

Supporting Information Available: Complete X-ray diffraction data for **3A**, **4A**, and **5**, including tables of atomic coordinates, thermal parameters, and bond lengths and angles, diagrams of the molecular structures with labeling schemes, and CIF files and text and figures detailing the syntheses and IR and NMR data of [Pt(BAB)(Me)(CO)][BAr′$_4$] and [Pt(BAM)(Me)(CO)][BAr′$_4$], syntheses, protonation reactions, and NMR spectra of [Pt(BAM)(*p*-PhEt)$_2$] and [Pt(BAB)(η^1-CH_2Ph)$_2$], and complete 1D NMR spectra with peak assignments and complete 2D NOESY NMR spectra of **3**, **4**, and **6**. This material is available free of charge via the Internet at http://pubs.acs.org.

OM0608861